Chemical Oscillators in Group VIA: The Cu(II)-Catalyzed Reaction between Hydrogen Peroxide and Thiosulfate Ion[1]

Miklós Orbán[2a] and Irving R. Epstein*[2b]

Contribution from the Institute of Inorganic and Analytical Chemistry, L. Eötvös University, Budapest, H-1443, Hungary, and Department of Chemistry, Brandeis University, Waltham, Massachusetts 02254. *Received July 29, 1986*

Abstract: In the presence of small amounts ($\sim 10^{-5}$ M) of Cu(II), the reaction between hydrogen peroxide and thiosulfate ion in a stirred tank reactor exhibits one oscillatory and three stationary states as well as bistability between the oscillatory and one of the stationary states and between two stationary states. The amplitude of the oscillations can be as large as 4 pH units or 200 mV in the potential of a Pt redox electrode. Near the bistable regions, the system undergoes large over- and undershoots as the flow rate is varied. In the absence of the copper catalyst, only a single steady state is found, with no unusual dynamical phenomena. Some tentative mechanistic suggestions are offered to account for this behavior.

Research on oscillating reactions and other exotic dynamical phenomena in chemistry has been confined until quite recently to reactions based on the chemistry of the halogen elements.[3] During the past several years, it has been found that similar behavior is possible in the oxidation–reduction reactions of the elements in groups IVA, VA, and VIA, elements which also support a wide range of oxidation states. Examples include oscillation in the cobalt and bromide-catalyzed air oxidation of benzaldehyde,[4] bistability in a variety of autocatalytic nitrate oxidations,[5] the oscillatory reaction of methylene blue, sulfite, sulfide, and oxygen[6] and the oxidation of sulfide ion by hydrogen peroxide.[7] Nevertheless, the state of development of complex dynamical phenomena in non-halogen systems remains quite primitive in comparison to our knowledge of such behavior in the reactions of the group VIIA elements.

In this paper we present a new bistable and oscillatory system involving the reaction of two common chalcogen compounds: the oxidation of thiosulfate ion by hydrogen peroxide catalyzed by trace amounts of Cu(II). If the reaction is carried out in an isothermal stirred tank reactor (CSTR), oscillations can occur in the pH as well as in the potential of either a platinum redox electrode or a Cu^{2+}selective electrode. Two types of bistability occur involving the steady states and the oscillatory state.

The catalyst-free H_2O_2–$S_2O_3^{2-}$ reaction has already been the subject of CSTR experiments by Chang and Schmitz.[8] Under quasiadiabatic conditions, thermokinetic oscillations with large amplitude temperature variations ($\Delta T \sim$ 10–20 °C) were found and explained in terms of the strong exothermicity of the reaction. No oscillations occur in the catalyst-free reaction in an isothermal CSTR.

The Cu(II)-catalyzed H_2O_2–$S_2O_3^{2-}$ system was studied in a closed (batch) configuration by Abel.[9] Cupric ion was shown to enhance the rate of the reaction significantly. No previous CSTR experiments have been carried out on the catalyzed reaction.

Experimental Section

Materials. Stock solutions were prepared from commercially available (Fisher Certified A.C.S.) H_2O_2 (30% solution), $Na_2S_2O_3 \cdot 5\,H_2O$, $CuSO_4$, H_2SO_4, and NaOH. Hydrogen peroxide solutions were prepared daily and kept in polyethylene bottles to retard decomposition. The H_2O_2 content was determined by $KMnO_4$ titration. The $CuSO_4$ stock solution (4×10^{-2} M) was stored in dilute (pH $\sim$ 4) H_2SO_4 to prevent hydrolysis. Dilutions were made with distilled water.

Apparatus. The plastic CSTR had a volume of 39.7 cm^3 and was operated in isothermal mode at a temperature of 25.00 ± 0.05 °C. The reactor was fed by a Sage 375A peristaltic pump through four inlet tubes (i.d. 2.5 mm). The flow rate (k_0 = (inflow volume per s)/(reactor volume) = τ^{-1}, where τ is the residence time) could be varied continuously between 0 and 1.3×10^{-2} s^{-1} with an accuracy of ±3%. The reactor was equipped with a bright platinum electrode of surface area $\sim$50 mm^2, a $Hg|Hg_2SO_4|K_2SO_4$ reference electrode (Radiometer P101), and a combined glass electrode (Orion, 91-04). In several experiments the combined glass electrode was replaced by an Orion Cu(II)-selective electrode. The Pt reference couple was connected to a double channel recorder (Linear 1200), while the glass electrode was connected to the second channel of the recorder through a digital pH meter (Orion 501 Digital Ionalyzer). The solution in the CSTR was stirred magnetically at about 600 rpm. The reactor was designed to avoid any air gap between the surface of the reaction mixture and the reactor cap.

Methods. Three of the four inlet tubes were used to introduce H_2O_2, $S_2O_3^{2-}$, and Cu(II) into the reactor. The fourth input channel carried the appropriate concentration of acid or base. When H_2SO_4 was introduced, as was the case in the majority of experiments, the Cu(II) and acid solutions were premixed and pumped in through a single tube in order to prevent hydrolysis of the very dilute Cu(II) during the course of the lengthy experiments. This precaution may have been unnecessary, since no difference was found in several parallel experiments with premixed and nonpremixed Cu(II) and H_2SO_4 solutions.[10]

The following concentration ranges were tested:

$$[H_2O_2]_0,\ 5 \times 10^{-2} - 5 \times 10^{-1}\ \text{M}$$

$$[S_2O_3^{2-}]_0,\ 1 \times 10^{-3} - 1 \times 10^{-1}\ \text{M}$$

$$[CuSO_4]_0,\ 1 \times 10^{-5} - 1 \times 10^{-4}\ \text{M}$$

$$[H_2SO_4]_0,\ 1 \times 10^{-5} - 1 \times 10^{-2}\ \text{M}$$

$$[NaOH]_0,\ 2.5 \times 10^{-3} - 2.5 \times 10^{-2}\ \text{M}$$

At a Cu(II) input concentration of about 1×10^{-4} M, a small amount of brownish precipitate is formed in the reactor and settles on the walls and on the electrode surfaces. The precipitate appears to be Cu_2S resulting from the slow side reaction[8]

$$2Cu^+ + S_2O_3^{2-} + H_2O \rightarrow Cu_2S + SO_4^{2-} + 2H^+$$

Apart from the brownish color at high $[Cu(II)]_0$, the solution in the reactor was always colorless and free of any visible precipitation.

Steady states, oscillations, and bistability were established, and phase diagrams were constructed by the techniques employed in earlier work.[7] Briefly, at each set of input concentrations the reactor was filled at the highest attainable flow rate. The flow rate was first decreased to zero and then increased back to the maximum in a stepwise fashion, pausing

(1) Paper 39 in the series Systematic Design of Chemical Oscillators. Paper 38: Luo, Y.; Epstein, I. R. *J. Chem. Phys.* **1986**, *85*, 5733.
(2) (a) Eötvös University. (b) Brandeis University.
(3) For reviews of halogen-based phenomena, see: *Oscillations and Traveling Waves in Chemical Systems*, Field, R. J.; Burger, M., Eds.; Wiley: New York, 1985.
(4) Jensen, J. H. *J. Am. Chem. Soc.* **1983**, *105*, 2639.
(5) Bazsa, G.; Epstein, I. R. *Comm. Inorg. Chem.* **1986**, *5*, 57.
(6) Burger, M.; Field, R. J. *Nature (London)* **1984**, *307*, 720.
(7) Orbán, M.; Epstein, I. R. *J. Am. Chem. Soc.* **1985**, *105*, 2302.
(8) Chang, M.; Schmitz, R. A. *Chem. Eng. Sci.* **1975**, *30*, 21.
(9) Abel, E. *Monatsh. Chem.* **1913**, *34*, 1361.
(10) For examples of systems in which premixing effects can be significant, see: ref 1 and Menzinger, M.; Boukalouch, M.; De Kepper, P.; Boissonade, J.; Roux, J. C.; Saadoui, H. *J. Phys. Chem.* **1986**, *90*, 313.

0002-7863/87/1509-0101$01.50/0

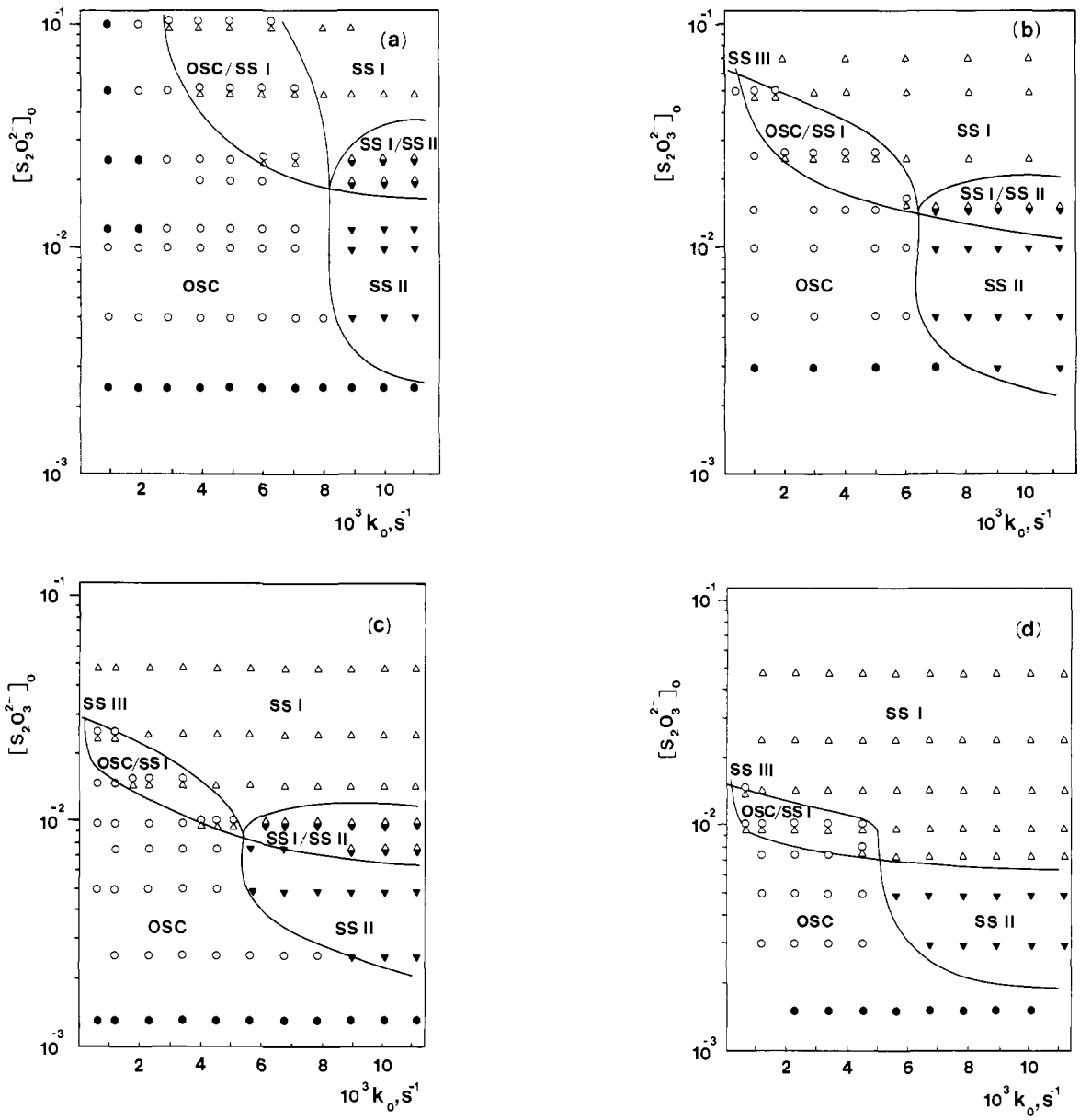

Figure 1. Phase diagram of the H_2O_2–$S_2O_3^{2-}$–Cu(II) system at 25 °C, with fixed constraints: $[Cu(II)]_0 = 2.5 \times 10^{-5}$ M, $[H_2SO_4]_0 = 0.001$ M. Four cuts parallel to the k_0–$[S_2O_3^{2-}]_0$ plane with $[H_2O_2]_0$ = (a) 0.5 M, (b) 0.25 M, (c) 0.1 M, and (d) 0.05 M. Symbols: ○, high (Δ pH > 0.5 units) amplitude oscillations; ●, low amplitude oscillations; △, SSI; ▼, SSII. SSIII appears at very low k_0 in a range too narrow to be shown on the figure.

at each value of k_0 to allow a stable state, stationary or oscillatory, to become established.

Results

Phase Diagrams. When H_2O_2 and $S_2O_3^{2-}$ solutions are introduced into the CSTR together with a catalytic amount of Cu(II), the system reaches and remains in one of four well-characterized states after an initial transient period. Three of these states are stationary; the fourth is oscillatory. The steady states may be distinguished by their pH and redox potential. SSI, the socalled flow branch, is characterized by a high pH (7–9) and a redox potential of 100 mV or more below that of SSII, which has a pH between 3.5 and 5. The thermodynamic branch, SSIII, is stable only at very low flow rates ($k_0 < 5 \times 10^{-4}$ s^{-1}) or in the absence of flow. It shows a lower pH (~3.5) and a higher redox potential than either of the other two steady states or the oscillatory state. The amplitude and frequency of the oscillatory state vary considerably with the conditions, but the oscillations always lie within the range $2.7 \leq$ pH ≤ 8.6 and have a redox potential amplitude of 10–200 mV, lying between 500 and 900 mV vs. SHE.

The experimental constraints, i.e., the temperature, the input concentrations, and the flow rate, determine which state will arise, except in regions of bistability, where the past history of the system decides which of the two possible stable states will occur. The behavior of the system as the constraints are changed is best summarized in a constraint–constraint or phase diagram such as that shown in Figure 1. Here we have fixed the temperature and the values of $[Cu(II)]_0$ and of $[H_2SO_4]_0$ and determined the state of the system at various $[H_2O_2]_0$ and $[S_2O_3^{2-}]_0$ as a function of flow rate. Figures 1a–d show four cuts through the full three-dimensional phase diagram at four different values of $[H_2O_2]_0$. Note the existence of regions of bistability in which either of two states can occur under the identical set of constraints. These "whale-tail" shaped regions shift and shrink, with the SSI–SSII finally disappearing entirely as $[H_2O_2]_0$ is decreased.

Since SSI and SSII differ considerably in pH and the pH undergoes large changes in the oscillatory state, significant variations in the states may be anticipated as the acidity of the input flow is varied. The results of such experiments are summarized in Figure 2, which shows the pH observed in the CSTR at different input concentrations of H_2SO_4 (Figure 2a,b) or NaOH (Figure 2c,d). At the extremes ($>2.5 \times 10^{-2}$ M) of high acid or base input, we observe steady states of low and high pH, respectively, regardless of the flow rate. As the input acid is decreased from an initial high value, SSII appears at high flow rates at $[H_2SO_4]_0 = 2.5 \times 10^{-3}$ M (Figure 2a, curve 3) and then gives way to large

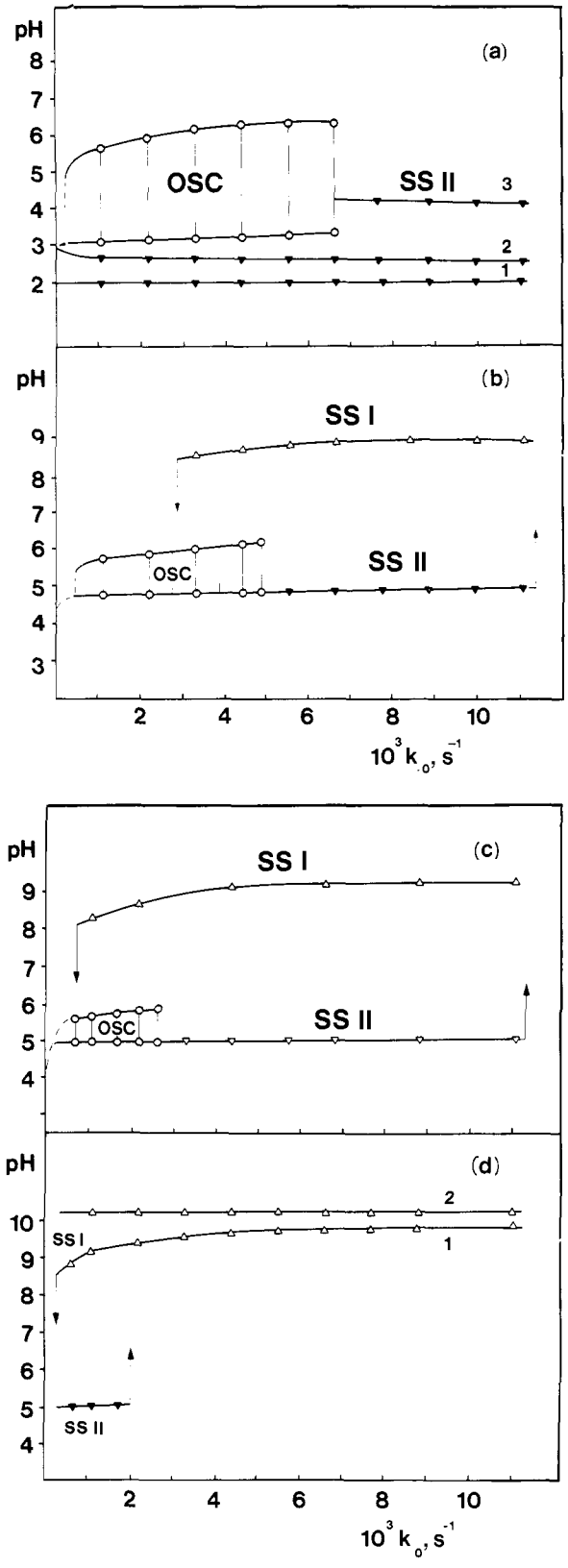

Figure 2. Change in the pH of the H_2O_2–$S_2O_3^{2-}$–Cu(II) system with k_0 and input acid or base concentration, with fixed constraints: $[Cu(II)]_0 = 2.5 \times 10^{-5}$ M, $[H_2O_2]_0 = 0.1$ M, $[S_2O_3^{2-}]_0 = 0.01$ M. Symbols as in Figure 1. $[H_2SO_4]_0$ = (a, curve 1) 1×10^{-2} M, (a, curve 2) 5×10^{-3} M, (a, curve 3) 2.5×10^{-3} M; (b) 1×10^{-4} M; $[NaOH]_0$ = (c) 2.5×10^{-3} M; (d, curve 1) 1×10^{-2} M, (d, curve 2) 2.5×10^{-2} M.

amplitude oscillations at $k_0 = 6.6 \times 10^{-3}$ s^{-1}. At an input acid concentration of 1×10^{-4} M (Figure 2b), the two forms of bistability appear, and the regions of bistability widen and shift toward lower k_0 as $[H_2SO_4]_0$ is lowered or is replaced by an inflow of base. Oscillations persist, though with lower amplitude, until

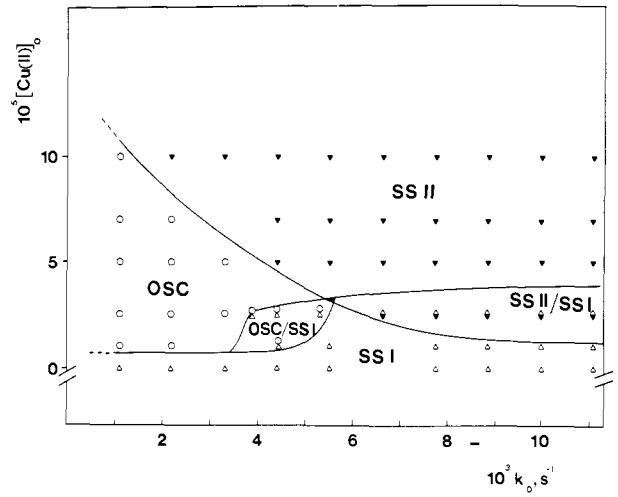

Figure 3. Phase diagram of the H_2O_2–$S_2O_3^{2-}$–Cu(II) system in the k_0–$[Cu(II)]_0$ plane, with fixed constraints: $[H_2SO_4]_0 = 0.001$ M, $[H_2O_2]_0 = 0.1$ M, $[S_2O_3^{2-}]_0 = 0.01$ M. Symbols as in Figure 1.

$[NaOH]_0 = 2.5 \times 10^{-3}$ M (Figure 2c). At still higher input pH (Figure 2d, curve 1), only the SSI–SSII bistability and the individual steady states remain, with the bistability disappearing for input base concentrations above 1×10^{-2} M (Figure 2d, curve 2).

Experiments were performed in which the H_2SO_4 or NaOH input was replaced with a buffer solution: pH 4 Fisher potassium biphthalate, pH 7 Fisher potassium phosphate monobasic–sodium hydroxide, or pH 10 Fisher potassium carbonate–potassium borate–potassium hydroxide. Runs were carried out at compositions and flow rates (e.g., at $[S_2O_3^{2-}]_0 = 0.025$ M, $k_0 = 3.5 \times 10^{-3}$ s^{-1} in Figure 1b or at $[S_2O_3^{2-}]_0 = 0.003$ M, $k_0 = 2.0 \times 10^{-3}$ s^{-1} in Figure 1d) where oscillations and/or bistability occur with acid or base instead of buffer as input. Under these conditions a buffer concentration of 0.05 M completely suppressed oscillations and bistability. Both the pH and the potential of the Pt electrode remained constant.

The addition of Cu(II), whose effects are shown in Figure 3, also has a dramatic influence on the behavior of the system. Without any Cu(II) there is a single steady state with a pH of 5.8 at high flow rates that increases slowly with decreasing k_0 and then drops more steeply to pH 3.6 as the flow rate approaches zero. From this observation and from the batch experiments to be discussed below, we conclude that, in the absence of the catalyst, the composition of the solution in the reactor is primarily determined by eq. (1), i.e., by the conversion of thiosulfate to tetrathionate, except under near-batch ($k_0 \sim 0$) conditions, where the oxidation of tetrathionate to sulfate becomes significant.

$$H_2O_2 + 2S_2O_3^{2-} \rightarrow S_4O_6^{2-} + 2OH^- \quad (1)$$

Addition of a small input flow of $CuSO_4$ markedly alters the behavior of the system. At $[Cu(II)]_0 = 1 \times 10^{-5}$ M, high amplitude oscillations appear at flow rates below 5×10^{-3} s^{-1}. Increasing the catalyst input concentration to 2.5×10^{-5} M causes the two regions of bistability to appear. As $[Cu(II)]_0$ is increased still further, we observe the disappearance of SSI and a narrowing and shift to lower k_0 and pH of the oscillatory region. The abovementioned precipitation of copper sulfide at catalyst inputs above 1×10^{-4} M prevented our following the reaction at higher Cu(II) concentrations.

Oscillations. The waveform of the oscillation changes markedly with the constraints. Two examples are given in Figures 4 and 5. The Pt electrode traces exhibit the greatest variation. At high $[H_2O_2]_0$ they tend to be simple relaxation oscillations of low amplitude (20–80 mV) and high frequency (2–6-min period) centered around a potential of 800–900 mV. Lower $[H_2O_2]_0$ and higher $[S_2O_3^{2-}]_0$ lead to more complex waveforms sometimes with two to four suboscillations per cycle, larger amplitude (100–200 mV) and longer period (10–20 min) about a lower (500–700 mV) average potential. While the oscillations vary considerably in

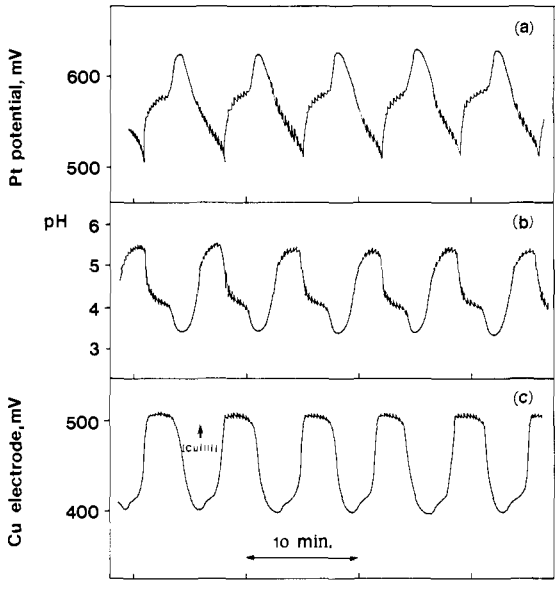

Figure 4. Oscillations in (a) potential of a Pt electrode (b) pH, (c) potential of a Cu(II)-selective electrode (increasing potential corresponds to increasing $[Cu^{2+}]$): $[H_2O_2]_0 = 0.25$ M, $[S_2O_3^{2-}]_0 = 0.025$ M, $[H_2SO_4]_0 = 0.0075$ M, $[Cu(II)]_0 = 2.5 \times 10^{-5}$ M, $k_0 = 3.35 \times 10^{-3}$ s^{-1}.

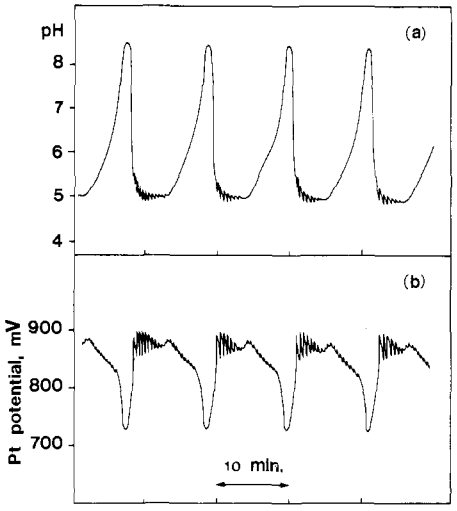

Figure 5. Oscillations in (a) pH, (b) potential of a Pt electrode: $[H_2O_2]_0 = 0.1$ M, $[S_2O_3^{2-}]_0 = 0.01$ M, $[H_2SO_4]_0 = 0.001$ M, $[Cu(II)]_0 = 2.5 \times 10^{-5}$ M, $k_0 = 4.5 \times 10^{-3}$ s^{-1}.

appearance as the constraints are changed, they appear to change continuously from one type to the other. We found no evidence for the existence of two different limit cycles or birhythmicity.[11]

The pH oscillations roughly follow the oscillations in redox potential but with less structure. High redox potential always corresponds to low pH and vice versa. The pH change can be as large as 3–4 units, particularly near the boundary between SSI and the oscillatory state, where the oscillations appear to carry the system between SSI and SSII. Under these conditions, one can induce periodic color changes by adding appropriate acid–base indicators to the input streams. At some combinations of lower $[S_2O_3^{2-}]_0$ and lower k_0, the amplitude of the pH oscillations is only 0.1–0.2 units, even though the redox potential varies by 10–80 mV.

A Cu^{2+}-selective electrode was also employed to monitor the oscillations. A typical trace is shown in Figure 4c. Although the electrode responds readily to changes in the state of the reaction mixture, we cannot draw quantitative conclusions from its potential, since both Cu(II) and thiosulfate ions influence its value.

(11) Alamgir, M.; Epstein, I. R. *J. Am. Chem. Soc.* **1983**, *105*, 2500.

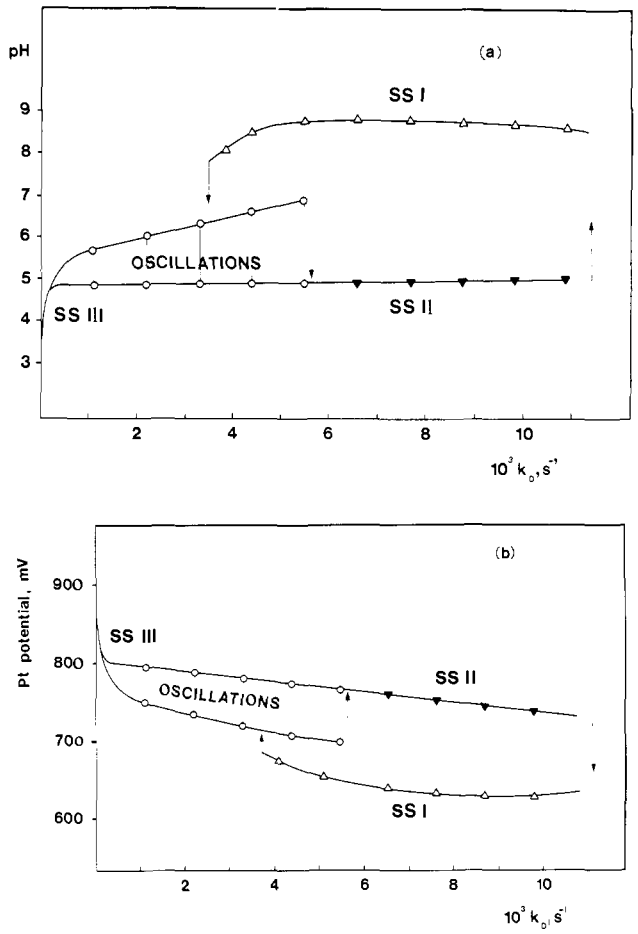

Figure 6. Constraint–response diagrams showing (a) pH and (b) Pt electrode potential vs. k_0 with $[H_2O_2]_0 = 0.1$ M, $[S_2O_3^{2-}]_0 = 0.01$ M, $[H_2SO_4]_0 = 0.001$ M, $[Cu(II)]_0 = 2.5 \times 10^{-5}$ M. Symbols as in Figure 1. Vertical segments in the oscillatory region indicate amplitudes of oscillation. arrows show k_0 values at which transitions occur.

The temperature in the reactor was monitored during the oscillations with a sensitive mercury thermometer. The temperature variation was found to be less than 10^{-2} °C per cycle, thereby excluding the possibility that the Cu(II)-catalyzed chemical oscillations discussed here are connected with the uncatalyzed thermokinetic oscillations reported by Chang and Schmitz.[8]

Bistability. The two types of bistability that occur in this system are best understood with the help of response–constraint diagrams such as those in Figure 6. This figure is equivalent to a horizontal section across the phase diagram of Figure 1c at the level $[Na_2S_2O_3]_0 = 10^{-2}$ M. At the highest accessible flow rate, the system is found in SSI. This state persists as k_0 is lowered until a flow rate of 3.5×10^{-3} s^{-1} is reached. The system then begins to oscillate, and, if the flow is decreased still further, the oscillations continue until the flow rate is nearly zero. At very low flow rates, the system undergoes a transition to SSIII. If k_0 is increased from the transition point at 3.5×10^{-3} s^{-1}, the system remains oscillatory until $k_0 = 5.5 \times 10^{-3}$ s^{-1} whereupon it switches to SSII. Further increases in flow rate leave the system in SSII up to the highest flow achievable with our pump. However, at high flow rates an appropriate perturbation, such as injection of a small amount of NaOH, can induce a transition from SSII to SSI. There are thus two regions of bistability: between SSI and the oscillatory state for $3.5 \times 10^{-3} < k_0 < 5.5 \times 10^{-3}$ s^{-1} and between SSI and SSII for k_0 between 5.5×10^{-3} s^{-1} and some upper limit that we are unable to determine because it exceeds our maximum pumping rate.

Figure 6 was obtained by varying k_0 in small increments (5×10^{-4} s^{-1} in the neighborhood of transitions and 1×10^{-3} s^{-1} in other regions). The system shows pronounced over- and undershoots when the flow rate is changed, and the magnitude of this phe-

nomenon increases both with the size of the change in k_0 and with proximity to a transition point. If Δk_0 is too large, the over- or undershoot can be large enough to induce a premature transition between two bistable states, thereby giving an erroneous value for the range of bistability. All state-to-state transitions were found to be quite rapid.

In regions of bistability, it is possible to perturb the system in such a way as to induce a change from one state to another without varying the bifurcation parameter (k_0) beyond the limits of bistability. This property is particularly useful in producing transitions that cannot otherwise be brought about because they occur at a flow rate beyond the capability of our pump. It is also a useful test for multistability. We summarize here the perturbations capable of inducing such transitions under the conditions of Figure 6

SSII → SSI

(a) addition of small amounts of NaOH ($\sim 10^{-3}$ M)

(b) rapid, single step increase in k_0 by more than 3×10^{-3} s^{-1}

SSI → SSII

temporarily stop pumping

SSII → oscillatory state

(a) addition of small amounts of H_2SO_4 ($\sim 10^{-3}$ M)

(b) rapid, single step increase in k_0 by more than 3×10^{-3} s^{-1}

(c) temporarily stop pumping

Oscillatory state → SSII

addition of small amounts of NaOH ($\sim 10^{-3}$ M)

Discussion

The kinetics and the products of the reaction between hydrogen peroxide and thiosulfate ion vary with the pH, the temperature, and any catalysts present in the reaction mixture.[12,13] In acetic acid–acetate buffer or dilute acid at room temperature, the major process is that given by eq 1 above. This reaction is claimed to be quantitative in dilute acetic acid solutions, with a rate law[14]

$$-\frac{d[H_2O_2]}{dt} = k_1[H_2O_2][S_2O_3^{2-}] + k_2[H_2O_2][S_2O_3^{2-}][H^+]$$

Edwards[15] gives $k_1 = 2.5 \times 10^{-2}$ M^{-1} s^{-1}, $k_2 = 1.7$ M^{-2} s^{-1}. Mechanisms involving the intermediates $HOS_2O_3^-$[14] and $HS_2O_3^-$[16] have been suggested. Some metal ions, such as Cu^{2+}, speed up the reaction significantly, but in dilute solution the stoichiometry remains unaffected.[9] This acceleration is proportional to the concentrations of H_2O_2 and Cu^{2+}, but is independent of both the thiosulfate and acid concentrations. The rate of the Cu-catalyzed process at 25 °C is (concentration units in M, time in min)

$$-\frac{d[H_2O_2]}{dt} = 1.53[H_2O_2][S_2O_3^{2-}] + 1 \times 10^3[H_2O_2][Cu^{2+}]$$

Abel[9] proposed that the catalyzed reaction involves a rapid initial process

$$2Cu^{2+} + 2S_2O_3^{2-} \rightarrow 2Cu^+ + S_4O_6^{2-}$$

followed by the slower process

$$2Cu^+ + H_2O_2 + 2H^+ \rightarrow 2Cu^{2+} + 2H_2O$$

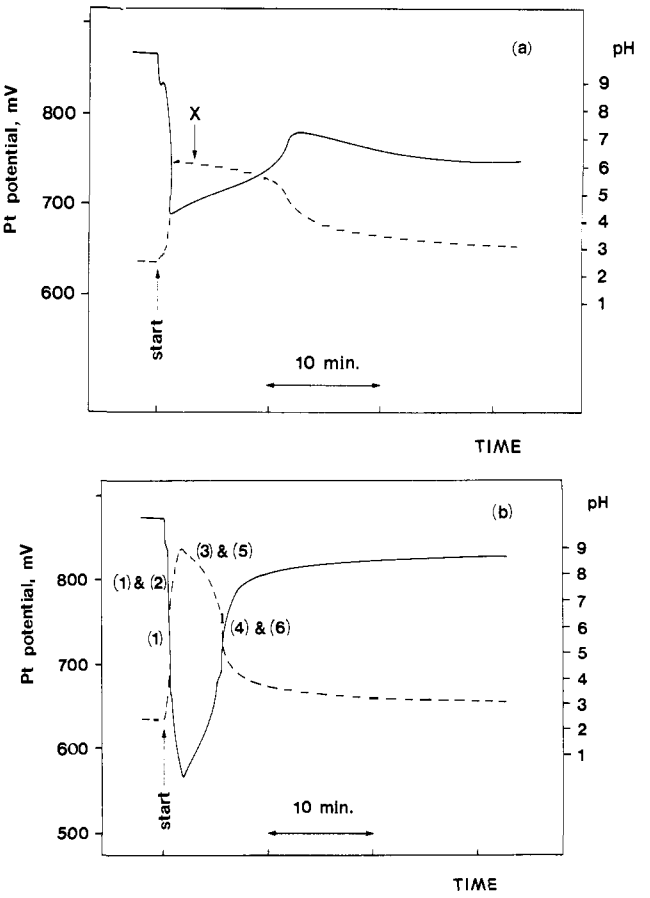

Figure 7. Batch experiments in which 0.1 M H_2O_2, 0.01 M $S_2O_3^{2-}$, and 0.001 M H_2SO_4 are reacted in the (a) absence and (b) presence of 2.5×10^{-5} M Cu(II). Dashed line, pH; solid line, Pt electrode potential. Numbers in parentheses along the dotted line indicate dominant processes (see text) during that portion of the reaction.

Yokosuka et al.[13] suggest that at pH > 4 reaction 2 begins to compete with reaction 1, producing trithionate as well as tetrathionate.

$$3S_2O_3^{2-} + 4H_2O_2 \rightarrow 2S_3O_6^{2-} + 2OH^- + 3H_2O \quad (2)$$

In neutral solution, the reaction yields a mixture of $S_4O_6^{2-}$, $S_3O_6^{2-}$ and SO_4^{2-}, while in alkaline solution the product is mainly sulfate, as a result of the reactions[13]

$$S_2O_3^{2-} + 4H_2O_2 \rightarrow 2SO_4^{2-} + 2H^+ + 3H_2O \quad (3)$$

$$S_3O_6^{2-} + 4H_2O_2 \rightarrow 3SO_4^{2-} + 4H^+ + 2H_2O \quad (4)$$

$$S_4O_6^{2-} + 7H_2O_2 \rightarrow 4SO_4^{2-} + 6H^+ + 4H_2O \quad (5)$$

No rate laws are available for reactions 3–5. Our own preliminary batch experiments suggest that they are all catalyzed to some extent by Cu(II).

In an attempt to determine which processes play major roles in the chemistry of the various states found in our flow experiments, we carried out a series of batch reactions. Figure 7 shows the pH and redox potential traces in a batch experiment with the same initial concentrations as the input to the CSTR in Figure 6, where both bistability and oscillations occur. In the absence of Cu(II) (Figure 7a) the H_2O_2–$S_2O_3^{2-}$ system shows a rapid initial rise in pH accompanied by a decrease in the potential of the Pt electrode. At a pH of about 6, the direction of change reverses, and the pH begins to decrease slowly while the redox potential increases. After about 10 min the rate of H^+ production increases, and we observe a sigmoidal drop in the pH and rise in the potential before the reaction approaches equilibrium.

With Cu(II) the reaction (Figure 7b) is more rapid and, presumably, more complex. The initial slope of the traces is steeper, and the pH rise continues to a value near 9; the potential drop

(12) *Gmelin's Handbuch der Anorganischen Chemie*; *8. Auflage, Schwefel, Teil B, Lieferung 2*; Verlag, Chemie GmbH: Weinheim/Bergstrasse, 1960; pp 904–907.
(13) Yokosuka, F.; Kurai, T.; Okuwaki, A.; Okabe, T. *Nippon Kagaku Kaishi* **1975**, 1901.
(14) Abel, E. *Monatsh. Chem.* **1907**, *28*, 1239.
(15) Edwards, J. O. *J. Phys. Chem.* **1952**, *56*, 279.
(16) Abel, E. *Monatsh. Chem.* **1950**, *81*, 798.

is also larger than in the copper-free case. After the extreme values are reached, the pH decrease and potential increase also occur more rapidly in the presence than in the absence of Cu(II).

Similar results are obtained if the copper-free reaction is allowed to proceed to point X in Figure 7a, and then Cu(II) is introduced. The pH then increases from about 6 to 9, and the traces show behavior very similar to that depicted in Figure 7b. We infer that the added Cu(II) enables the oxidation of $S_2O_3^{2-}$ via eq 1 and 2 to proceed further toward completion before the intermediates, and $S_4O_6^{2-}$ and $S_3O_6^{2-}$ are converted to sulfate by eq 4 and 5 resulting in the drop to a final pH of about 3.5.

Batch experiments on the H_2O_2 oxidation of sodium tetrathionate were also carried out with and without added Cu(II). At initial pH 2.5, there was no observable reaction either in the presence or the absence of catalyst. At pH 4.7, we find a very slow decrease in pH, to about 4.2 in 10 min, suggesting a slow oxidation of $S_4O_6^{2-}$ to SO_4^{2-}. A starting pH of 6.4 gives a final value of 3.9 within 5 min. Higher initial pH's give even more rapid reaction, with a pH drop of about 3.4 units occurring in 2 min or less. The shapes of the pH traces resemble the descending portion of Figure 7b. No transient pH increase took place in any $S_4O_6^{2-}$ oxidation. We conclude that $S_4O_6^{2-}$ is stable to attack by H_2O_2 below pH 4 but is oxidized according to eq 5 at increasingly greater rates as the pH increases above 4.

The initial portion of the reaction, whether or not Cu(II) is present, is dominated by reaction 1. In the absence of the catalyst, this reaction is overtaken at pH $\sim$ 6 by the direct oxidation of $S_2O_3^{2-}$ to SO_4^{2-}, eq 3, and by the oxidation of $S_4O_6^{2-}$, eq 5. As a result, the solution then becomes acidic.

In the presence of Cu(II) reaction 1 and possibly reaction 2 as well are accelerated, so that more thiosulfate is consumed and more OH^- is produced before the production of sulfate and H^+ becomes dominant. Förster and Hornig[17] report that trithionic acid hydrolyzes in weakly acidic or weakly basic solution according to

$$H_2S_3O_6 + H_2O \rightarrow H_2SO_4 + H_2S_2O_3 \quad (6)$$

The hydrolysis is greatly accelerated by salts of copper.

We have summarized in Figure 7b the major reactions occurring during each portion of the batch H_2O_2–$S_2O_3^{2-}$–Cu(II) reaction. We now attempt to explain the chemistry underlying the dynamical behavior of this system in the CSTR.

The uncatalyzed H_2O_2–$S_2O_3^{2-}$ reaction results in a steady state whose composition is determined primarily by the stoichiometry of reaction 1. The major sulfur-containing species present are $S_4O_6^{2-}$ and unreacted $S_2O_3^{2-}$. As the flow rate approaches zero, reaction 3 may also come into play, producing some sulfate ion and lowering the pH. Lack of any autocatalysis or other complex feedback precludes the possibility of bistability and/or oscillation.

The H_2O_2–$S_2O_3^{2-}$–Cu(II) system shows bistability and oscillation. The presence of the catalyst induces a much larger pH rise as a result of the acceleration of reaction 1 and possibly also reaction 2. The steady-state SSI has a composition derived from eq 1 and 2. It represents, as shown by the low Pt potential and high pH, the "most reduced" stable composition of the system. This state is favored by lower H^+ and Cu(II) inputs. SSII may be characterized by reactions 3, 4, and 6. Reaction 5 is of no significance at the stationary pH of SSII. Higher $[H^+]_0$ and $[Cu(II)]_0$ tend to give rise to SSII. Oscillations require a match between the input concentrations and the flow rate so that reactions 1–6 may be switched on and off at appropriate points in the cycle by the H^+ and OH^- that are generated by the individual steps. When the system is in oscillation and approaching the pH minimum, reactions 3 and 4 dominate, consuming OH^-. However, as the system becomes more acidic, the rate of these reactions decreases, and reactions 1 and 2 begin to take over, producing $S_4O_6^{2-}$, $S_3O_6^{2-}$, and OH^-. At the pH maximum, reactions 1 and 2 shut down as first reaction 5 and then reactions 3, 4, and 6 are switched on.

The H_2O_2–$S_2O_3^{2-}$–Cu(II) system may thus be regarded as a pH-regulated oscillator in which the component reactions separately produce and consume $[H^+]$, thereby turning each other on and off by cross-coupling. The Cu(II) accelerates several of the processes enough to enable the system to reach extreme values of pH at which one set of reactions (1–2 or 3–5) dominates the other. The switch from one extreme to the other is generated by the product (H^+ or OH^-) inhibition of the reactions. The ability of input buffer solutions to suppress bistability and oscillations argues strongly that the pH plays a critical role in the dynamical behavior of the system rather than simply serving as an indicator of that behavior. The fact that within a narrow range of conditions the system can undergo oscillations with a pH amplitude of only 0.1–0.2 units (the Pt potential oscillations are still sizeable) still remains to be explained.

In addition to providing one of a handful of examples of a Group VIA oscillator, the present system may also constitute a useful analogue of the chlorite–thiosulfate reaction,[18] an oscillator that exhibits a variety of exotic dynamical phenomena including complex oscillation,[19] chemical chaos,[19] and wave propagation.[20] Like chlorite, hydrogen peroxide is found in a large number of chemical oscillators and is able to act either as an oxidant or as a reductant. Perhaps some of the insights gained in studying the H_2O_2–$S_2O_3^{2-}$–Cu(II) system will shed light on the perplexing mechanism of the ClO_2^-–$S_2O_3^{2-}$ oscillator.

Acknowledgment. This work was supported by the National Science Foundation (CHE8419949) and by a U.S.–Hungarian Cooperative Grant from the NSF (INT8217658) and the Hungarian Academy of Sciences.

(17) Förster, F.; Hornig, A. *Zeit. Anorg. Chem.* **1925**, *142*, 119; Förster, F. *Zeit. Anorg. Chem.* **1925**, *144*, 337.

(18) Orbán, M.; De Kepper, P.; Epstein, I. R. *J. Phys. Chem.* **1982**, *86*, 431.

(19) Orbán, M.; Epstein, I. R. *J. Phys. Chem.* **1982**, *86*, 3907.

(20) Nagypál, I.; Bazsa, G.; Epstein, I. R. *J. Am. Chem. Soc.* **1986**, *108*, 3635.